

Polymer Crystallinity (A survey of polymer crystallization by X-ray diffraction . chapter 10)

|       |   |
|-------|---|
| メタデータ | 言語: en<br>出版者: SKP<br>公開日: 2008-01-31<br>キーワード (Ja):<br>キーワード (En):<br>作成者: Asano, Tsutomu, Mina, Md. Forhad<br>メールアドレス:<br>所属: |
| URL   | <a href="http://hdl.handle.net/10297/557">http://hdl.handle.net/10297/557</a>   |

## Chapter 10. Polymer Crystallinity

### 10.1 Introduction

The concept of crystallinity of a polymer was applied by a two-phase assumption consisting either of a complete crystalline or of a complete amorphous state. By a recent development of the polymer morphology, the two-phase concept became inconsistent with the discovery of folded chains or paracrystalline states, which belong to the intermediate orders. However, as a result of increasing experimental evidence, confidence and convenience of the crystallinity based on the two-phase model were reestablished. The crystallinity is now generally accepted as a basic factor of polymer morphology.

In the previous chapter, the crystallinity,  $\alpha_c$ , is derived from the density measurement. We define here the value of  $w_c$ , as a crystallinity measured by X-ray diffraction method. Determination of  $w_c$  of polymer materials was widely performed by means of various methods [1-7]. Among them, the Ruland method [6] is a universal one including a concept of crystalline distortion. The crystallinity is derived by comparison between total and crystalline intensities. This method was further developed by Vonk [8] by a computer processing.

For evaluation of the crystallinity, it is necessary to consider that the crystal contains lattice distortions. In case of polymers, there are two distortions known as the first-kind (type I) and the second-kind (type II). While the type-I disorder arising from thermal motion with a long-range order, the type-II has a paracrystalline order suggested by Hosemann [9]. In the theory of crystallinity measurements, the disorder function of the type-I is usually employed in the Ruland, Vonk and other modified methods [6, 8, 10-13].

In the section 10.2, we describe the determination of  $w_c$  and  $k$  during initial crystallization of PET. Based on the crystallinity measurement by Gehrke and Zachmann [14], the fitting method was modified for PET [10]. In the section 10.3, we discuss separation of the two distortions by the modified method of Vonk [15,16]. In this chapter, we consider further possibility in the crystallinity measurement by the modified methods.

### 10.2 Crystallinity and Crystal Distortion of PET

#### 10.2.1 Preparation and characterization of PET samples

The PET samples were synthesized from terephthalic acid dimethylester and ethylene glycol as described by Günther and Zachmann [17] with antimony and calcium acetate as catalysts. The degree of crystallinity and the amount of lattice distortion were obtained from WAXS patterns. The temperatures and times of polycondensation of the sample are listed in Table 10.1, where we designate the sample containing calcium acetate by C, that containing manganese acetate by M, and the sample without catalyst by O. The synthesized samples are melt-pressed and then quenched in ice-water. The glassy PET is crystallized by annealing at temperature  $T_a$  for  $t_a$  sec.

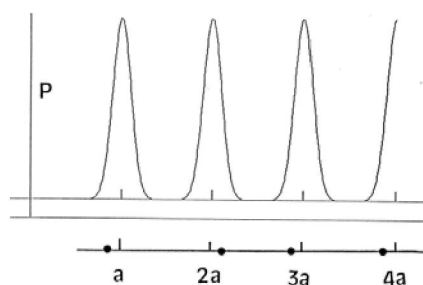
Table 10.1 Description of samples investigated [10]

| Sample | Catalyst          | Polycondensation |            |
|--------|-------------------|------------------|------------|
|        |                   | Temperature (°C) | Time (min) |
| M      | Manganese acetate | 270              | 30         |
| C      | Calcium acetate   | 270              | 45         |
| O      | No catalyst       | 285              | 210        |

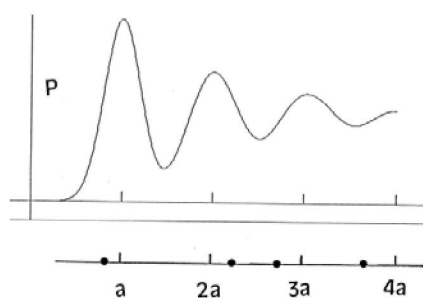
### 10.2.2 WAXS measurements

The degree of crystallinity,  $w_c$  and the lattice distortion factor  $k$  were determined by evaluation of the WAXS profiles. The measured curves were corrected for the air scattering, the polarization factor and the absorption factor, and then multiplied by  $s^2$  ( $s = 2 \sin \theta/\lambda$ ). The curves were normalized by adding the atomic scattering factor for the coherent scattering,  $f_{\text{coh}}^2(s)$ , and for the Compton scattering,  $f_{\text{inc}}^2(s)$ , averaged over the different atoms. Then the Compton scattering was subtracted.

We consider two kinds of disorders illustrated in Fig.10.1. The type I disorder has a long range order, whereas the type II order appears rather short range. For the present fitting method, we usually consider the type I disorder caused by thermal motions.



(a) First-kind (type I) disorder



(b) Second-kind (type II) disorder

Fig.10.1 One dimensional disorder-models as a function of lattice constant  $a$ .  
 $P$  displays the probable electron density distribution around the origin.

### 10.2.3 Background calculation for the fitting method

For evaluation of the WAXS curve, the Ruland method [6] has been slightly modified. A background scattering,  $I_{\text{back}}$ , caused by the amorphous regions and the crystal imperfections has been calculated by means of the equation.

$$s^2 I_{\text{back}} = w_c s^2 f_{\text{coh}}^2(s) (1 - e^{-ks^2}) + (1 - w_c) s^2 I_{\text{amorph}}(s) \dots \dots \dots (10.1)$$

where  $w_c$  is the crystallinity,  $f_{\text{coh}}^2(s)$  is the averaged atomic scattering factor for coherent scattering, and  $k$  is the distortion factor of the first order lattice distortion [6, 10]. The first term of Eq.(10.1) is the contribution from diffuse scattering of the distorted crystal. Different values for  $w_c$  and  $k$  ( $\text{nm}^2$ ) were assumed for calculation. The second term is the amorphous scattering, where  $I_{\text{amorph}}(s)$  is measured from a quenched PET.

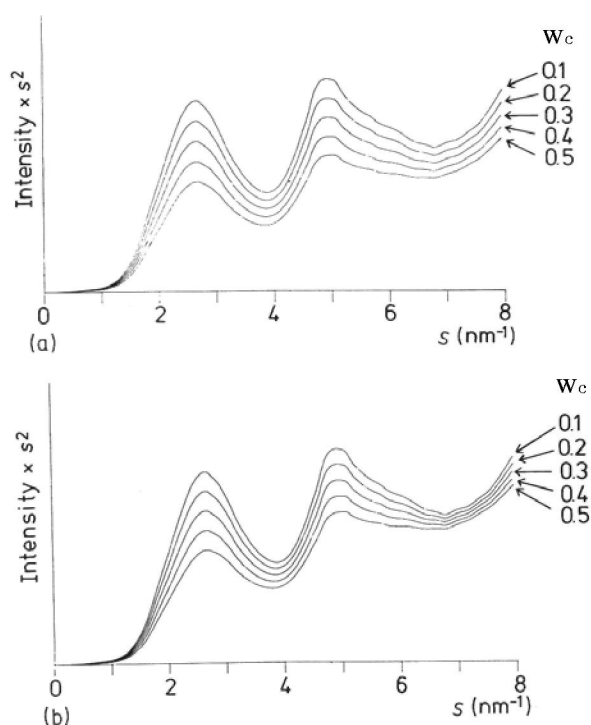


Fig. 10.2 Normalized background scattering caused by the amorphous regions and crystal imperfections of PET as a parameters of  $w_c = 0.1 \sim 0.5$ , for values of  $k$ : (a)  $k = 0.01$ , (b)  $k = 0.02$  ( $\text{nm}^2$ ) [10].

Figure 10.2(a) shows  $I_{\text{back}}$  calculated in the case of  $k = 0.01$ , assuming at different  $w_c$  varying from 0.1 to 0.5. Figure 10.2(b) shows the corresponding results in the case of  $k = 0.02$ . By increase of  $w_c$  at a constant  $k$ ,  $I_{\text{back}}$  is shifted downwards. On the other hand,  $I_{\text{back}}$  shifts to higher by increasing  $k$ .

In order to evaluate the measured WAXS curves of PET samples, the calculated curves were fitted to the measured ones. For this purpose, the observed intensity is correctly normalized. Then, the observed curve was compared to the calculated background. It is

necessary to choose the best fit region in the special scattering reason  $s$ . These regions are different by the substance, because the crystalline scattering disturbs the fitting. In the case of PET, we use the four intervals  $s = 1.4$  to  $1.6$ ,  $s = 2.1$  to  $2.3$ ,  $s = 4.0$  to  $4.2$  and  $s = 7.4$  to  $7.6$   $\text{nm}^{-1}$ . As indicated in Fig.10.3, these fitting regions are most sensitive to measure crystallinity of PET. Then,  $w_c$  and  $k$  were determined when  $I_{\text{exp}}$  and  $I_{\text{back}}$  show the best fit.

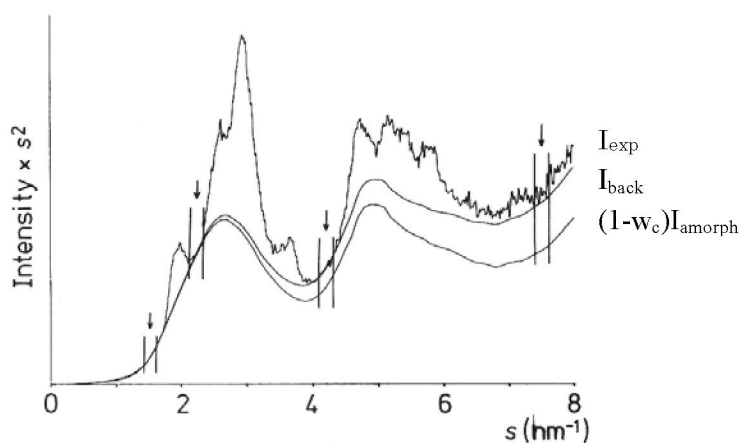


Fig. 10.3 Comparison of measured intensity ( $I_{\text{exp}}$ ), calculated background scattering ( $I_{\text{back}}$ ) and amorphous scattering ( $I_{\text{amorph}}$ ).  $I_{\text{exp}}$  is obtained by the sample M crystallized for 80 sec at  $T_c = 130^\circ\text{C}$  [10].

The result for sample M crystallized at  $130^\circ\text{C}$  for 80 min is shown in Fig.10.3. The best fit of the background curve is obtained at  $w_c = 0.32$  and  $k = 0.022$ . Consequently, the amorphous intensity is obtained by  $I_{\text{amorph}} \times 0.68$ . The difference between  $I_{\text{back}}$  and the amorphous intensity is attributed to the lattice distortion. As seen in Fig.10.3, the effect of the distortion does not appear on the fitting regions at lower  $s$  ( $s = 1.4$  to  $1.6$ ,  $s = 2.1$  to  $2.3$ ). Accordingly, we determine  $w_c$  by the best fit of these regions.

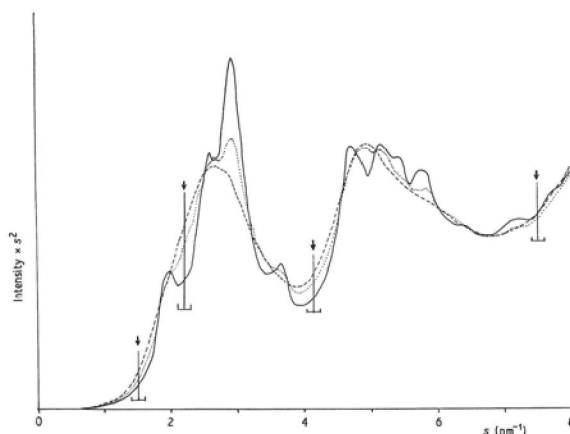


Fig. 10.4 Normalized WAXS profiles of sample M crystallized at  $130^\circ\text{C}$  for (---) 60 sec, (.....) 80 sec and (—) 80 min [10].

### 10.2.4 Comparison of $w_c$ and $k$

Figure 10.4 shows the WAXS curves of sample M crystallized at 130 °C. The degree of crystallinity becomes larger with increasing crystallization time. The fitting regions are marked by arrows. In the region  $s=1$  to 5  $\text{nm}^{-1}$ , the scattered intensity is lowered with increasing crystallization time, but all curves are at the same level in the region  $s > 6 \text{ nm}^{-1}$ . This result shows that the amount of lattice distortion becomes larger with increasing crystallization time.

Figure 10.5 represents the WAXS profiles for different samples all crystallized at 110 °C for 60 min. The degrees of crystallinity are nearly the same for all samples. However, differences in the scattered intensity at  $s > 6 \text{ nm}^{-1}$  are observed. This fact indicates that the amount of lattice distortion is low in the sample C, medium in the sample M and high in the sample O.

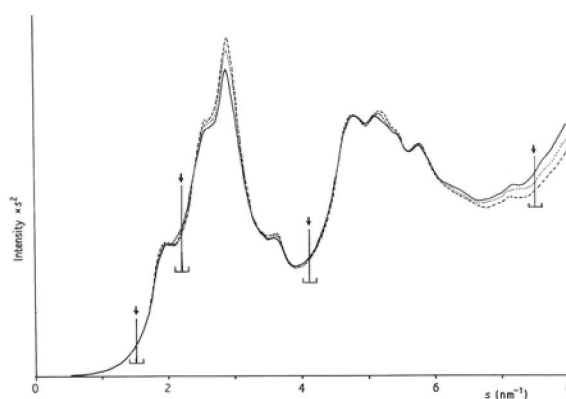


Fig. 10.5 Normalized WAXS profiles of (—) sample O, (····) sample M, and (---) sample C [10].

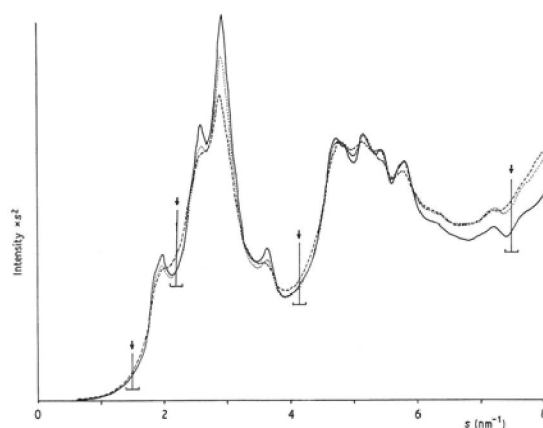


Fig. 10.6 Normalized WAXS curves of sample O for 60 min at (---) 110 °C, (····) 125 °C, and (—) 150 °C [10].

The effect of  $T_c$  measured by sample O is demonstrated in Fig. 10.6. The value of  $w_c$  increases with increasing  $T_c$ . The scattered intensity at  $s > 6 \text{ nm}^{-1}$  is the smallest for  $T_c=150 \text{ °C}$ , which indicates the least amount of  $k$  at this crystallization temperature.

The results of crystallinity ( $w_c$ ) derived from WAXS are summarized in Table 10.2. With all samples,  $k$  becomes larger with increasing crystallization time. At  $T_c=110$  and  $125$  °C, the lowest  $k$  value appears for sample C and the highest one for sample O. For all samples,  $k$  decreases with increasing  $T_a$ .

The change of  $k$  as a function of  $w_c$  is shown in Fig. 10.7. In all the samples,  $k$  becomes larger with increasing  $w_c$  up to  $w_c=0.3$  and then decrease. In the region of increasing  $k$ , sample C shows the lowest while sample O shows the highest value.

The crystallinity from the density ( $\alpha_c$ ) is measured by Eq.(4.5) of chapter 4. The both crystallinities,  $\alpha_c$  and  $w_c$ , are compared in Table 10.2.

Table 10.2 Results of the crystallinity and lattice distortion by the fitting method [10]

| Sample | Crystallization     |         | Crystallinity<br>(WAXS),<br>$w_c$ | Lattice<br>Distortion<br>( $\text{nm}^2$ ) | Crystallinity<br>(density),<br>$\alpha_c$ |
|--------|---------------------|---------|-----------------------------------|--|---|
|        | Temperature<br>(°C) | Time    |                                   |  |   |
| C      | 130                 | 10 sec  | 0.09                              | 0.003                                      | 0.06                                      |
| C      | 130                 | 20 sec  | 0.22                              | 0.016                                      | 0.22                                      |
| C      | 130                 | 80 min  | 0.33                              | 0.022                                      | 0.28                                      |
| M      | 130                 | 60 sec  | 0.05                              | 0.009                                      | 0.06                                      |
| M      | 130                 | 80 sec  | 0.11                              | 0.016                                      | 0.13                                      |
| M      | 130                 | 80 min  | 0.32                              | 0.022                                      | 0.32                                      |
| O      | 130                 | 150 sec | 0.04                              | 0.010                                      | 0.06                                      |
| O      | 130                 | 300 sec | 0.22                              | 0.022                                      | 0.19                                      |
| O      | 130                 | 80 min  | 0.32                              | 0.022                                      | 0.28                                      |
| C      | 110                 | 60 min  | 0.28                              | 0.016                                      | 0.26                                      |
| M      | 110                 | 60 min  | 0.27                              | 0.018                                      | 0.24                                      |
| O      | 110                 | 60 min  | 0.23                              | 0.020                                      | 0.19                                      |
| C      | 125                 | 60 min  | 0.33                              | 0.020                                      | 0.30                                      |
| M      | 125                 | 60 min  | 0.33                              | 0.025                                      | 0.29                                      |
| O      | 125                 | 60 min  | 0.33                              | 0.025                                      | 0.27                                      |
| C      | 150                 | 60 min  | 0.36                              | 0.013                                      | 0.32                                      |
| M      | 150                 | 60 min  | 0.36                              | 0.013                                      | 0.32                                      |
| O      | 150                 | 60 min  | 0.37                              | 0.013                                      | 0.31                                      |
| C      | 110                 | 300 sec | 0.22                              | 0.013                                      | 0.20                                      |
| M      | 110                 | 300 sec | 0.26                              | 0.016                                      | 0.21                                      |
| O      | 110                 | 300 sec | 0.22                              | 0.022                                      | 0.20                                      |

### 10.2.5 Amount of lattice distortion

At 130 °C,  $k$  increases with increasing crystallization time. At 125 and 110 °C,  $k$  strongly depends on the catalyst: showing the highest value for sample O and lowest for sample C. Thus, the lattice distortion  $k$  will decrease depending on the catalyst. From these results, the  $k$  is related to the spherulite growth during the initial crystallization.

In the process of crystallization, the molecular packing becomes dense. At temperatures near  $T_g$ , the molecular mobility is limited and insufficient to form perfect orders. In the spherulitic growth, the crystal includes disorders with increasing distance from the nucleus.

By the above consideration,  $k$  increases with crystallization time by the fact that the radii of the spherulites become larger with time. The catalyst reduces  $k$  because the size of the spherulite is reduced by the nucleation.

At 150 °C,  $k$  is not depend on the catalyst, indicating that distortion is relaxed by increasing molecular movility.

Thus, we have two competing conclusions:

- i)  $k$  increases with the distance from the nucleus.
- ii)  $k$  decreases with the increasing thermal motion.

At low temperatures, the first effect is effective because of the limited thermal motions. At higher temperatures, the second process occurs simultaneously with the first one.

The fitting method is a traditional way to measure the crystallinity. However, *the finer determination is possible by choosing the best fitting region for the specific substance*. In the case of PET, the fitting method is effective in the initial crystallization having low  $w_c$  values.

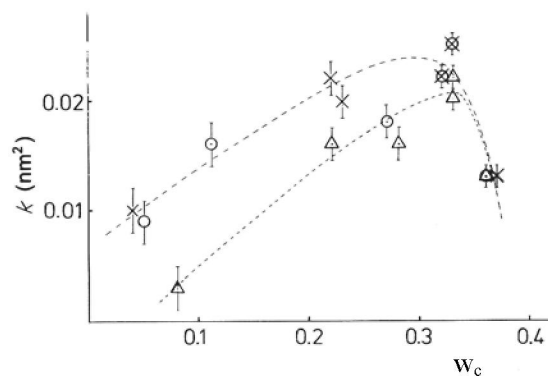


Fig. 10.7 Lattice distortion factor  $k$  as a function of the degree of crystallinity  $w_c$ : (Δ) sample C, (○) sample M, (×) sample O [10].

## 10.3 Theoretical Development of Crystallinity Measurement

### 10.3.1 Methods of Ruland and Vonk

According to Ruland, crystallinity by the X-ray diffraction method is defined by the following equation [6]:

$$W_c = \frac{\int_{s_0}^{s_p} s^2 I_c(s) ds}{\int_{s_0}^{s_p} s^2 I(s) ds} \cdot \frac{\int_{s_0}^{s_p} s^2 \bar{f}^2 ds}{\int_{s_0}^{s_p} s^2 \bar{f}^2 D(s) ds} \dots\dots\dots (10.2)$$

where  $s$  is the reciprocal vector ( $s = 2 \sin\theta/\lambda$ ),  $I(s)$  and  $I_c(s)$  are total and crystalline diffraction intensities of the measured angle (from  $s = s_0$  to  $s = s_p$ ), respectively.  $\bar{f}^2$  is given by:

$$\bar{f}^2 = \frac{N_i f_i^2}{N_i} \dots\dots\dots (10.3)$$

where  $f_i$  is a scattering factor of an atom of element  $i$ , and  $N_i$  is a number of the atom in the given molecule.  $D(s)$  is a disorder function defined by:

$$D_1(s) = e^{-ks^2} \dots\dots\dots (10.4)$$

$$D_2(s) = \frac{2e^{-2ks^2}}{1 + e^{-2ks^2}} \dots\dots\dots (10.5)$$

where  $D_1(s)$  and  $D_2(s)$  are first- and second-kind disorder functions, respectively, and  $k$  is a distortion factor. ( In the section 10.3, we discuss  $k$  in the range of  $\text{\AA}^2$ .)

If we represent:

$$R(s_p) = \frac{\int_{s_0}^{s_p} s^2 I ds}{\int_{s_0}^{s_p} s^2 I_c ds} \dots\dots\dots (10.6)$$

$$K(s_p) = \frac{\int_{s_0}^{s_p} s^2 \bar{f}^2 ds}{\int_{s_0}^{s_p} s^2 \bar{f}^2 D(s) ds} \dots\dots\dots (10.7)$$

then, we can write:

$$R(s_p) = \frac{K(s_p)}{w_c} \dots\dots\dots (10.8)$$

For a practical calculation, an approximation is used as follows:

$$K(s_p) = 1 + 0.5ks_p^2 \dots\dots\dots (10.9)$$

Then, Eq. 10.8 becomes

$$R(s_p) = \frac{1 + 0.5ks_p^2}{w_c} \dots\dots\dots (10.10)$$

If we plot the experimental value of  $R(s_p)$  versus  $s_p^2$ , we can determine  $w_c$  and  $k$  from the values of  $R(0)$  [an intercept of the ordinate of  $R(s_p)$ ] and  $R'(0)$  [a slope of the  $R(s_p)$  curve at  $s_p = 0$ ].

### 10.3.2 Modified Vonk's method

In order to compare the two types of disorders, the values of  $K(s_p)$  are computed for the both disorders by Eqs.(10.4) and (10.5). We consider here the approximation of  $K(s_p)$  by using  $b(k, s_p)$  [15,16]:

$$b(k, s_p) = (K(s_p) - 1) / k s_p^2 \dots\dots\dots (10.11)$$

where the value of  $K(s_p)$  are calculated from Eq. (10.7) for both disorders.

For the analytical calculations, we consider that  $f^2 = z^2$  at  $s_p = 0$ , where  $z$  is a total electron numbers in a molecule. Thus,

$$K(s_p) = \frac{z^2 \int_0^{s_p} s^2 ds}{z^2 \int_0^{s_p} s^2 D(s) ds} = \frac{\int_0^{s_p} s^2 ds}{\int_0^{s_p} s^2 D(s) ds} \dots\dots\dots (10.12)$$

Here, we compare two disorder functions shown by Eqs.(10.4) and (10.5). It is possible to calculate the value of  $K$  on the limit  $s_p \rightarrow 0$ .

For the type I (first-kind) disorder, we use Eq.(10.4).

$$\begin{aligned} \lim_{s_p \rightarrow 0} K(s_p) &= \lim_{s_p \rightarrow 0} \frac{\int_0^{s_p} s^2 ds}{\int_0^{s_p} s^2 \exp(-ks^2) ds} = \lim_{s_p \rightarrow 0} \frac{\int_0^{s_p} s^2 ds}{\int_0^{s_p} s^2 (1 - ks^2) ds} \\ &= \lim_{s_p \rightarrow 0} \frac{\int_0^{s_p} s^2 ds}{\int_0^{s_p} s^2 ds - ks^4 ds} = \lim_{s_p \rightarrow 0} \frac{\frac{s_p^3}{3}}{\frac{s_p^3}{3} - \frac{ks_p^5}{5}} \\ &= \lim_{s_p \rightarrow 0} \frac{1}{1 - \frac{3ks_p^2}{5}} = 1 + 0.6ks_p^2 \dots\dots\dots(10.13) \end{aligned}$$

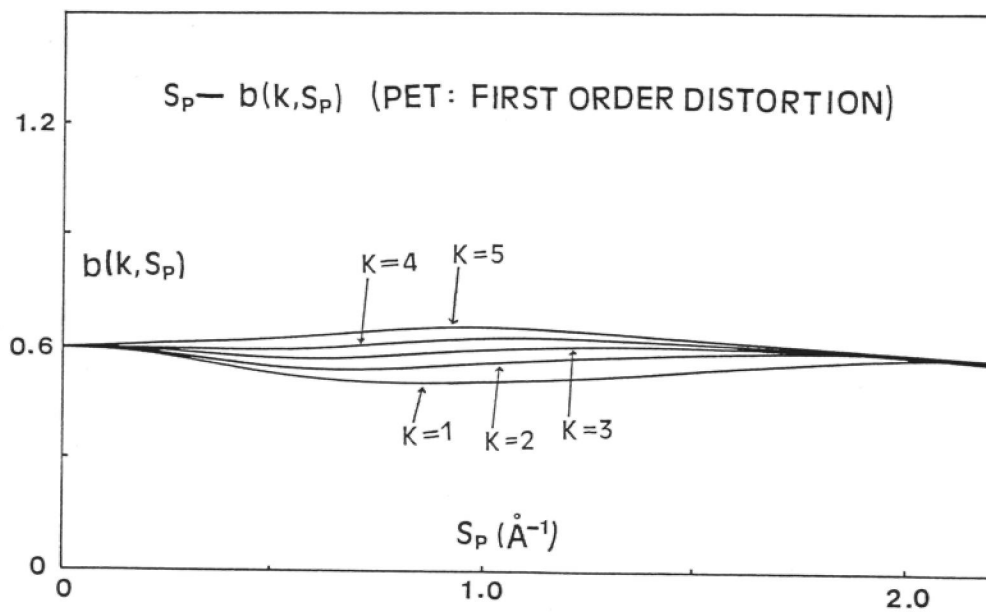
For the type II (second-kind) disorder, we use Eq.(10.5).  
On the limit  $s_p \rightarrow 0$ ,

$$\begin{aligned} D_2(S) &= \frac{2 \exp(-2ks^2)}{1 + \exp(-2ks^2)} = \frac{2}{1 + \exp 2ks^2} \\ \lim_{s \rightarrow 0} D_2(S) &= \lim_{s \rightarrow 0} \frac{2}{1 + (1 + 2ks^2)} = \lim_{s \rightarrow 0} \frac{1}{1 + ks^2} = 1 - ks^2 \dots\dots\dots(10.14) \end{aligned}$$

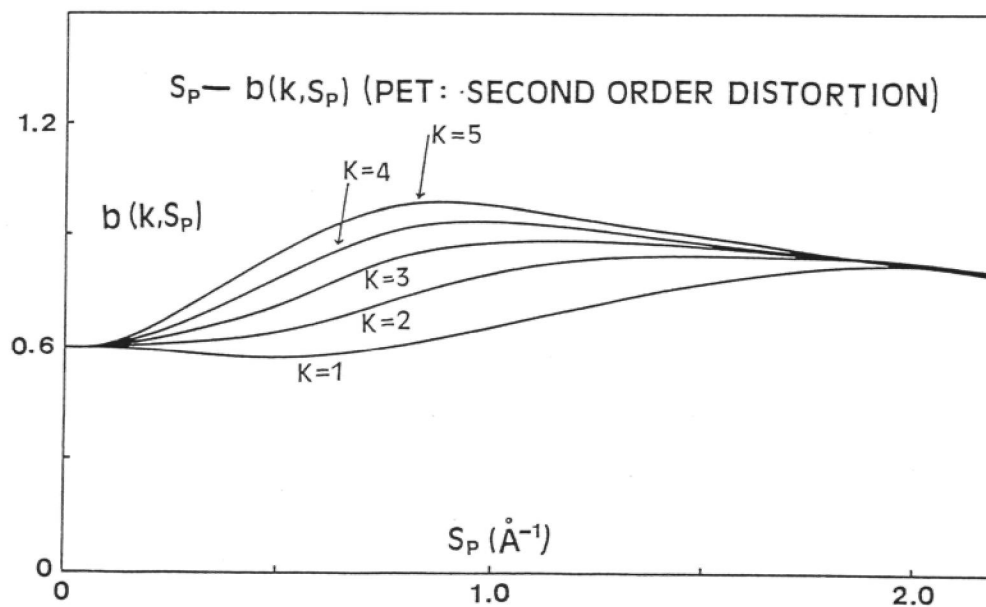
This limit of the type II shows the similar result as calculated on the type I.  
Then at the limit  $s_p \rightarrow 0$ , the b value approaches to 0.6 in the both distortions.

**10.3.3 Calculation of b(k,s<sub>p</sub>)**

From Eq.(10.11), b is changed by a parameter of k. It is possible to calculate the b value as a function of  $s_p$  (Å<sup>-1</sup>). The example of  $s_p$  - b(k,s<sub>p</sub>) curves are shown in Fig.10.8 for PET. The curve is shifted by a parameter of k, while  $k = 1 \sim 5$  (Å<sup>2</sup>) [15,16].



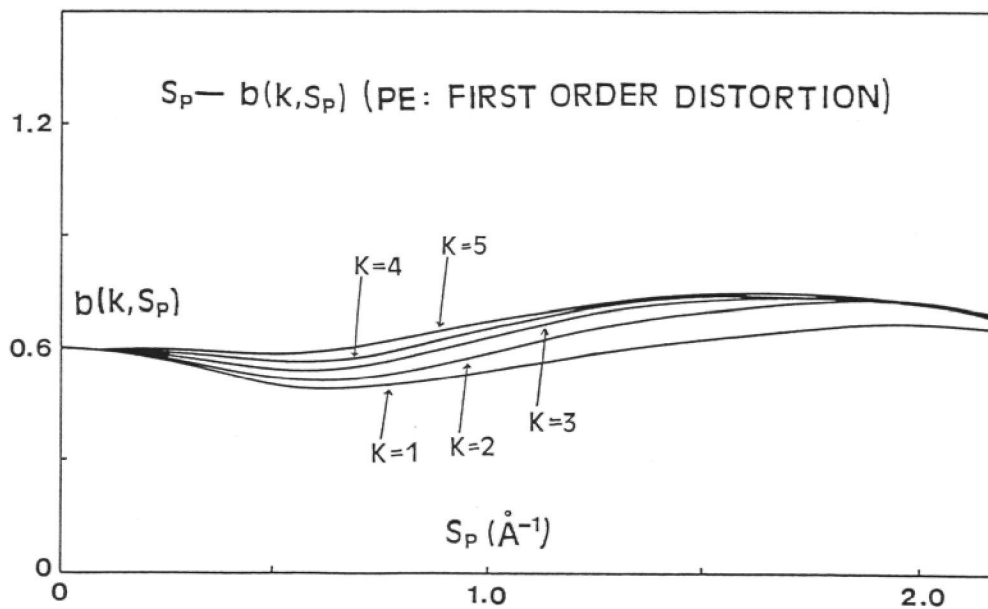
(a)



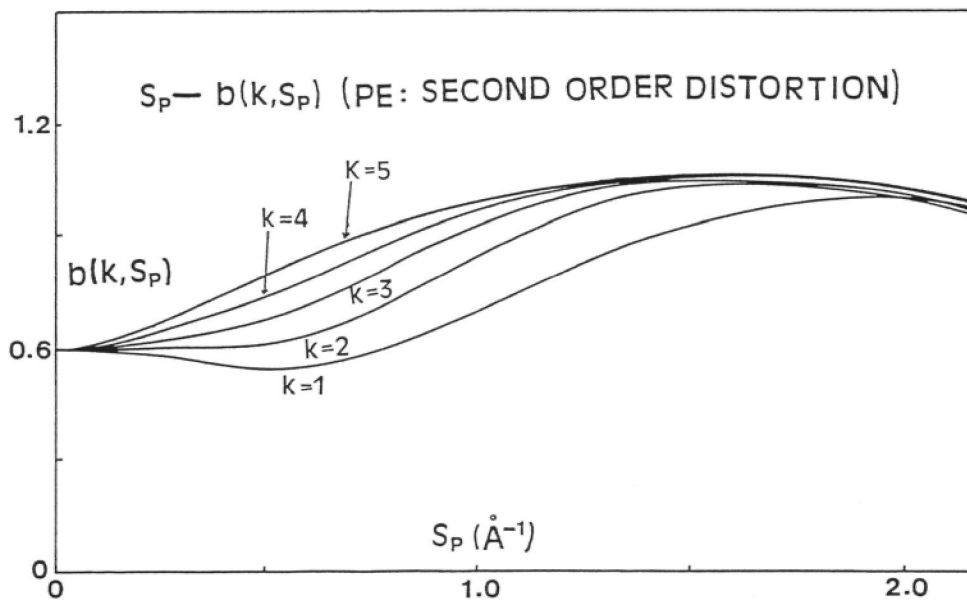
(b)

Fig. 10.8  $b$  values versus  $s_p$  for the case of PET, calculated by  
 (a) the first-kind disorder and (b) the second-kind disorder [15].

In Fig. 10.9, the example of  $s_p - b(k, s_p)$  curves are shown for PE.



(a)



(b)

Fig. 10.9  $b$  values versus  $s_p$  for the case of PE, calculated by (a) the first-kind disorder and (b) the second-kind disorder [15].

### 10.3.4 Evaluation by the modified Vonk's method

#### (i) Determination of the crystallinity and the lattice distortion factor

The initial values of  $w_c$  and  $k$  are determined from the experimental value of  $R(s_p)$  by the same procedure of the Vonk's method. However, we use the following equation.

$$R(s_p) = \frac{1 + 0.6ks_p^2}{w_c} \dots\dots\dots (10.15)$$

Plotting the experimental value of  $R(s_p)$  versus  $s_p^2$ , we draw a reasonable parabolic line through the oscillating  $R(s_p)$  curve. Then, the values of  $R(0)$  (the intercept of the ordinate of the parabola) and  $R'(0)$  (slope of the parabola at  $s_p = 0$ ) are measured by extrapolation. The initial values of  $w_c$  and  $k$  are determined by:

$$w_c = 1/R(0) \text{ and } k = w_c R'(0)/0.6 \dots\dots\dots (10.16)$$

#### (ii) Curve fitting to search the best value of $x_c$ and $k$

In the analysis by Eq.(10.16), it is difficult to find the best values of  $R(0)$  and  $R'(0)$  because of oscillation of the  $R(s_p)$  curve by the crystalline peaks in the region from  $s_p = 0$  to  $s_p = 1$ . It is possible to find out the best values of  $w_c$  and  $k$  by fitting the experimental  $b_{ex}$  value to the theoretical  $b$  value. The fitting method enables to use the overall experimental curve to determine the best values of  $w_c$  and  $k$ .

The fitting is performed by the following procedure:

- 1) The initial values of  $w_c$  and  $k$  are determined by Eqs (10.15) and (10.16).
- 2) The value of  $b_{ex}(s_p)$  is calculated from  $R(s_p)$  by putting in the initial values to the following equation.

$$b_{ex}(s_p) = \frac{w_c R(s_p) - 1}{ks_p^2} \dots\dots\dots (10.17)$$

- 3) Plotting the  $b_{ex}$  on the theoretical  $b$  (Figs 10.8 or 10.9).
- 4) The best fit of  $b_{ex}$  to the theoretical  $b$  can be found by shifting the values of  $w_c$  around the initial values.

### 10.3.5 Examples of the evaluation

The fitting procedures have been examined for the WAXS data. The examples of the best fit analyzed by PET and PE are displayed in Figs.10.10 and 10.11. In Fig. 10.10, the result obtained from PET shows that the crystalline disorder should have a characteristic of the first kind (type I). On the other hand, in the cases of PE, the best fitting in Fig. 10.11 occurs in the second kind disorder (type II).

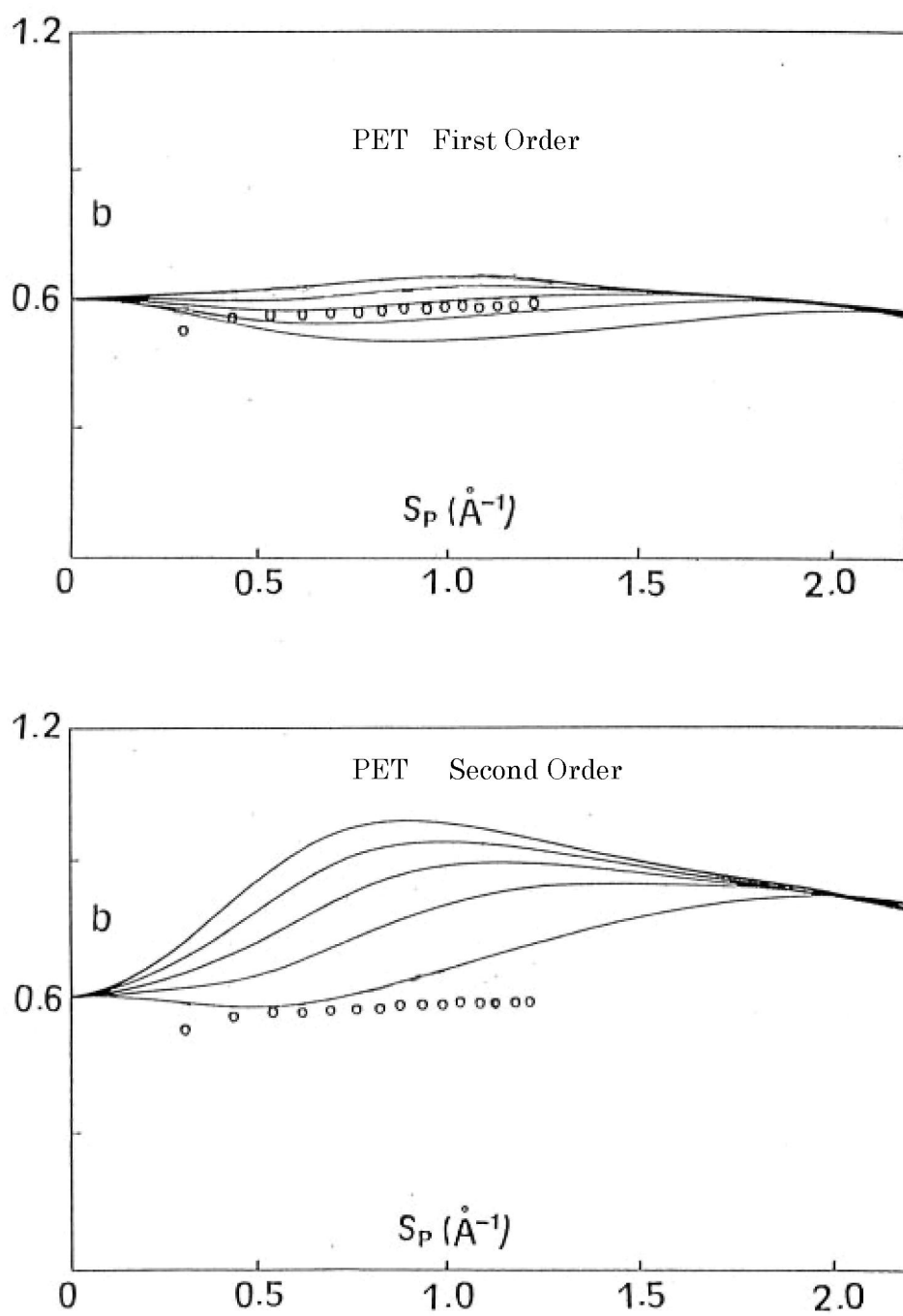


Fig. 10.10 Evaluation of  $b_{\text{ex}}$  from WAXS measurement of PET [15].  
 (○) Best fit of the evaluation shows  $w_c = 0.36$ ,  $k=2.5(\text{\AA}^2)$ .  
 The best fit appears in the first-kind disorder.

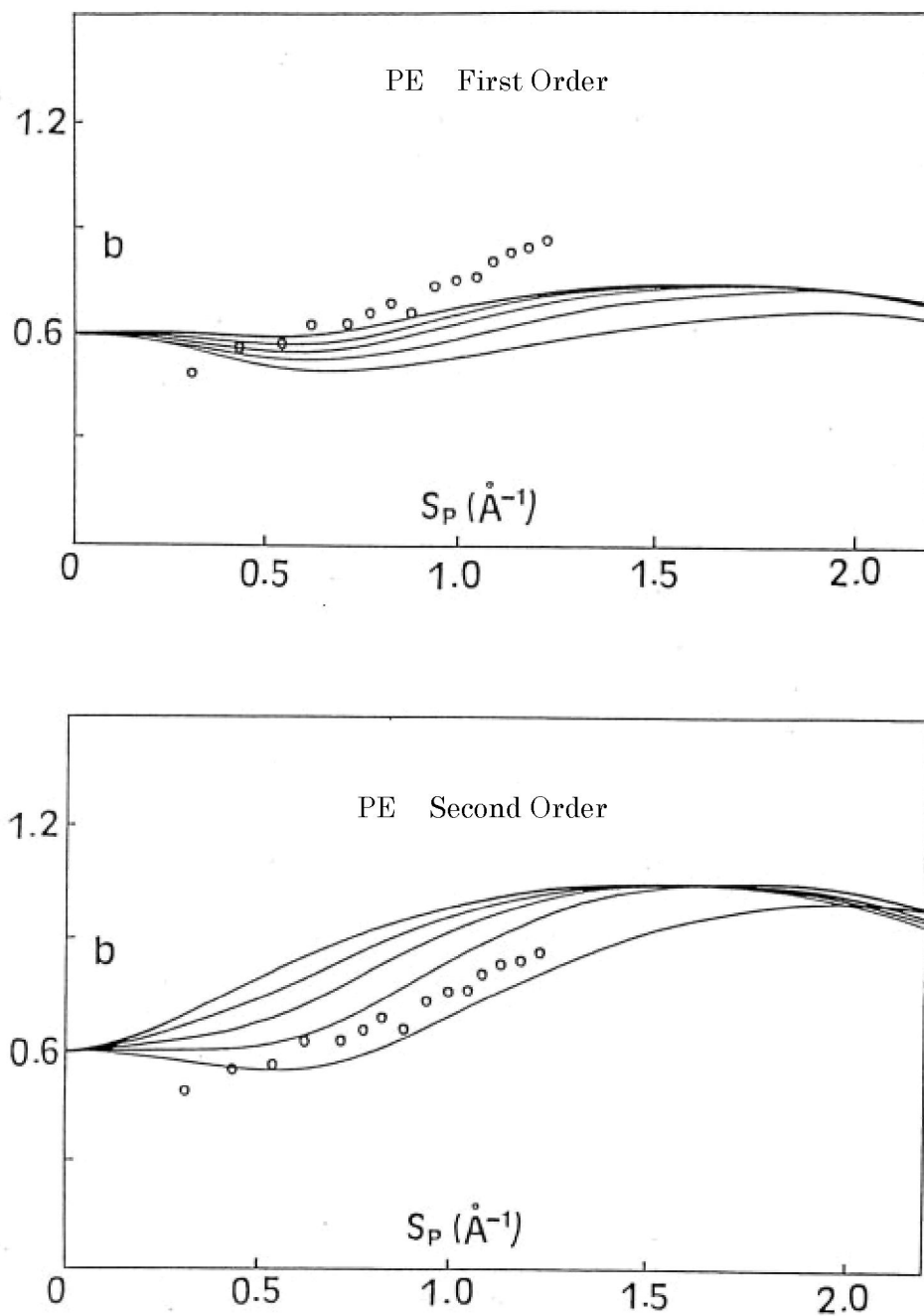


Fig. 10.11 Evaluation of  $b_{\text{ex}}$  from WAXS measurement of PE [15].  
 ( $\circ$ ) Best fit of the evaluation shows  $w_c = 0.43$ ,  $k=1.3(\text{\AA}^2)$ .  
 The best fit appears in the second-kind disorder.

### 10.3.6 Discussion

In the Vonk's method,  $w_c$  and  $k$  are determined from the extrapolation of  $R(s_p)$  at  $s_p=0$ . However, it is difficult to fix the best extrapolation, because of the oscillation of the  $R(s_p)$  in the range  $s_p < 1$ . Small shift of the extrapolation makes large difference in  $w_c$  and  $k$ .

*The present fitting method is advantageous on employing the whole experimental curve to determine  $w_c$  and  $k$ .* The extrapolated value can be corrected by choosing the best fit of the  $b_{ex}$  value.

Moreover, *the new fitting method enables us to separate the disorders.* It is possible to estimate the type of disorders by the modified Vonk's method. In case of mixtures of the two, it may be possible to estimate the ratio of two disorders. However, thinking about the basic approximation of the two-phase system (amorphous and crystal), precise separation becomes low significance in the polymer crystallinity.

## References

1. J. M. Goppel, *Appl. Sci. Res.* **A1**, 3 (1947)
2. L. E. Alexander, S. Ohlberg, G. R. Taylor, *J. Appl. Phys.* **26**, 1068 (1955)
3. J. H. Wakelin, H. S. Virgin, and E. Crystal, *J. Appl. Phys.* **30**, 11654 (1959)
4. P. H. Hermans and A. Weidniger, *Makromol. Chem.*, **50**, 98 (1961)
5. H. Hendus and G. Schnell, *Kunstst.*, **51**, 69 (1961)
6. W. Ruland, *Acta Cryst.* **14**, 1180 (1961)
7. W. O. Statton, *J. Appl. Polym. Sci.*, **7**, 803 (1963)
8. C. G. Vonk, *J. Appl. Cryst.*, **6**, 148 (1973)
9. R. Hosemann, *Acta Cryst.*, **4**, 520 (1951)
10. T. Asano, A. Dzeick-Pickuth and H.G. Zachmann, *J. Mater. Sci.*, **24**, 1967 (1989)
11. S. Polizzi, G. Fagherazzi, A. Benedetti, M. Battagliarin and T. Asano, *J. Appl. Cryst.* **23**, 359 (1990)
12. T. Asano, S. Nakahiro, T. Shiozawa and H.G. Zachmann, *Rep. Fac. Sci., Shizuoka Univ.*, **24**, 35-38 (1990)
13. S. Polizzi, G. Fagherazzi, A. Benedetti, M. Battagliarin and T. Asano, *Euro. Polym. J.*, **27**, 85-87 (1991)
14. R. Gehrke, and H. G. Zachmann, *Makromol. Chem.* **182**, 627 (1981)
15. T. Suzuki, *Master Dissertation, Fac. Sci., Shizuoka Univ. (in Japanese)* (1991)
16. T. Asano, T. Suzuki, S. Polizzi, H. G. Zachmann, *Macromol. Symp., Hamburg* (1990)
17. B. Günther and H. G. Zachmann, *Polymer* **24**, 1008, (1983)